LAWRENCE
LIVERMORE
NATIONAL
LABORATORY

LLNL-JRNL-660060

Lenard-Balescu Calculations and Classical Molecular Dynamics Simulations of Electrical and Thermal Conductivities of Hydrogen Plasmas

H. D. Whitley, C. R. Scullard, L. X. Benedict, J. I. Castor, A. Peters, J. N. Glosli, D. F. Richards, M. P. Desjarlais, F. R. Graziani

September 9, 2014

Contributions to Plasma Physics

Disclaimer

Lenard-Balescu calculations and classical molecular dynamics simulations of electrical and thermal conductivities of hydrogen plasmas

[1]Heather D. Whitley, [1]Christian R. Scullard, [1]Lorin X. Benedict,
[1]John I. Castor, [1]Amanda Randles, [1]James N. Glosli, [1]David
F. Richards, [2]Michael P. Desjarlais, and [1]Frank R. Graziani
[1]*Lawrence Livermore National Laboratory, Livermore, CA 94550, USA and*
[2]*Sandia National Laboratory, Albuquerque, NM 87185, USA*

(Dated: November 17, 2014)

Abstract

We present a discussion of kinetic theory treatments of linear electrical and thermal transport in hydrogen plasmas, for a regime of interest to inertial confinement fusion applications. In order to assess the accuracy of one of the more involved of these approaches, classical Lenard-Balescu theory, we perform classical molecular dynamics simulations of hydrogen plasmas using 2-body quantum statistical potentials and compute both electrical and thermal conductivity from our particle trajectories using the Kubo approach. Our classical Lenard-Balescu results employing the identical statistical potentials agree well with the simulations. Comparison between quantum Lenard-Balescu and classical Lenard-Balescu for conductivities then allows us to both validate and critique the use of various statistical potentials for the prediction of plasma transport properties. These findings complement our earlier MD/kinetic theory work on temperature equilibration [1], and reach similar conclusions as to which forms of statistical potentials best reproduce true quantum behavior.

I. INTRODUCTION

There is now a heightened interest in the transport properties of dense plasmas, owing to work in support of inertial confinement fusion (ICF) research at the National Ignition Facility [2]. Of particular interest is the thermal conductivity of both the DT (deuterium-tritium) fuel and the ablator material (typically comprised of low-Z elements like C, H, and Be). This is because large temperature gradients are predicted to be present in the neighborhood of certain interfaces separating material regions with markedly different densities, and the precise magnitudes of ∇T in these regions are therefore thought to have a large effect on the development of (unwanted) fluid instabilities [3]. Existing models for the thermal conductivities of the constituent materials exist for exactly these purposes [4–6], but they are based on a combination of ad hoc hypotheses and empirical fits to experimental data taken in regimes often quite far from those visited in ICF [7, 8].

Recently, there has been a spate of *ab initio* calculations of the electrical and thermal conductivities of dense plasmas in the precise regime of interest [9–12]. However, these approaches suffer from serious difficulties as T is increased into the keV realm due to the large number of high-energy states which much be included. The primary advantages of these density functional theory (DFT)-based approaches are three-fold: 1. The quantum nature of the electron-ion scattering is treated naturally, without the need to apply cut-offs as in the Coulomb-logarithm paradigm [13, 14], described below. 2. The artificial distinction of bound vs. free electrons is eliminated, allowing a plasma with a distribution of charge states to be described in a self-consistent, realistic manner. 3. Electron degeneracy is accounted for, enabling a proper description of the dense cold fuel in an ICF implosion scenario.

In this article, we employ an altogether different simulation approach, that of classical molecular dynamics (MD) with quantum statistical potentials (QSPs), which treats the quantum Coulomb scattering problem in an approximate way. This approach has been used extensively to model the static properties of dense plasmas [15–19], as well as certain dynamical properties such as temperature equilibration [17, 20, 21]. QSP-MD is free from the disadvantage of having to sum over numerous partially-occupied states as in the DFT-MD treatment of conductivities. We use QSP-MD to compute electrical and thermal conductivities of dense but non-degenerate hydrogen plasmas. These conductivities are computed in equilibrium simulations using the Kubo fluctuation-dissipation methodology [22]. Be-

cause different choices for QSPs exist, none of which were designed specifically to compute dynamical quantities like conductivities, we compare our results to those of the state-of-the-art plasma kinetic treatment: Lenard-Balescu theory [23], in which plasma screening enters through a multi-component dynamical dielectric function. By evaluating conductivities using both quantum and classical variants of Lenard-Balescu theory, we address the question: How well do we expect QSP-MD to do in predicting plasma transport in hydrogen, at least in the weak-coupling limit where kinetic theory can be trusted? This same strategy has been used to study the efficacy of QSP-MD for the simulation of electron-ion temperature equilibration [1]. In what follows, we review the history of plasma theories describing transport in our regime of interest (II A), present our scheme for making predictions to compare to our QSP-MD results (II B), describe our MD simulations (III), and discuss our findings (IV).

II. THEORY

We begin by reviewing the theory of linear transport in plasmas, specifically those kinetic theory treatments which have been developed to handle the regimes of interest to ICF ($\rho \sim 0.1 - 1000$ g/cc, T up to a few keV). In particular, we focus on kinetic theories aimed at addressing the weak-coupling limit, since these theories (beginning with that of Ref.[13]) have played an important role in the development of models in wide use for ICF and related applications. At the end of this section, we outline our basic strategy for solving the Lenard-Balescu equation in the perturbative manner needed for the prediction of linear transport, leaving many of the details for a subsequent manuscript [12].

A. General considerations

We focus on the contribution of the electrons to the conductivities, since they are thought to be the dominant contributors, given the large mass ratio, $m_{\text{proton}}/m_{\text{electron}}$. Assuming linear response to external perturbations, the charge ($\mathbf{j}_Z$) and heat ($\mathbf{j}_Q$) currents are related to the electric field and temperature gradient by [24]:

$$\mathbf{j}_Z = -\frac{1}{e}\left(-eL_{ZZ}\mathbf{E} + \frac{L_{ZQ}\nabla T}{T}\right)$$

$$\mathbf{j}_Q = -\frac{1}{e}\left(-eL_{QZ}\mathbf{E} + \frac{L_{QQ}\nabla T}{T}\right). \tag{1}$$

The electrical (σ) and thermal ($K_{\rm th}$) conductivities are related to the Onsager coefficients, L_{ab} [24]:

$$\sigma = L_{ZZ}, \tag{2}$$

and

$$K_{\rm th} = \frac{1}{T}\left(L_{QQ} - \frac{L_{ZQ}^2}{L_{ZZ}}\right). \tag{3}$$

The determination of σ and $K_{\rm th}$ then follows from the calculation of the currents $\mathbf{j}_Z$ and $\mathbf{j}_Q$ in the presence of the driving forces, $\mathbf{E}$ and ∇T. In a kinetic theory treatment, these currents are computed from the perturbed electron distribution function.

For simplicity, we describe kinetic theories which govern the evolution of a phase space distribution function, $f(\mathbf{r}, \mathbf{v}, t)$. This is only strictly meaningful for classical particles, since both $\mathbf{r}$ and $\mathbf{v}$ are simultaneously specified, but a straightforward generalization to the quantum case is possible using the Wigner distribution function [25]. The kinetic equation obeyed for the electron distribution function is:

$$\frac{\partial f}{\partial t} + \frac{\mathbf{F}}{m}\cdot\nabla_{\mathbf{v}} f + \mathbf{v}\cdot\nabla_{\mathbf{r}} f = C[f], \tag{4}$$

where $\mathbf{F}$ denotes an external force on the electrons and $C[f]$ is the collision operator, equal to the total time derivative of f and discussed at length below. For steady-state problems, such as those of electrical and thermal conductivity, the first term on the LHS is zero. To study the electrical conductivity of a homogeneous (on average) plasma, we set the third term on the LHS to zero as well, and set $\mathbf{F} = -e\mathbf{E}$ in the second term. The resulting equation, $(-e\mathbf{E}/m)\cdot\nabla_{\mathbf{v}} f = C[f]$, describes the steady-state electron distribution, f, in the presence of an electric field, $\mathbf{E}$. What remains is to specify a collision term. Once this is done and the resulting equation is solved, the DC electrical conductivity, σ, is given by Ohm's Law: $\mathbf{j}_Z = \sigma\mathbf{E}$, for a constant field $\mathbf{E}$. The electrical current density is simply

$$\mathbf{j}_Z = \int d^3v \mathbf{v} f(v). \tag{5}$$

For the BGK collision term (relaxation time approximation) [26], $C[f] = (f_0 - f)/\tau$, one obtains the familiar $\sigma = ne^2\tau/m$ [27], where f_0 is the equilibrium (e.g. Maxwellian) distribution, $n = \int d^3v f$ is the number density of electrons, and τ is a mean collision time [4]. It is important to note that the equilibrium distribution, f_0, gives rise to $\mathbf{j}_Z = 0$, since $f_0(\mathbf{v})$

is spherically symmetric. Thus, it is the non-spherical part of the steady-state solution to Eq.4 which contributes to the conductivity.

The thermal conductivity problem is a bit more subtle for three reasons: 1. The energy current involves contributions from potential energy in addition to the kinetic piece which depends only on $\mathbf{v}$. 2. Depending on the assumptions made, both the second and the third terms on the LHS of Eq.4 can be nonzero, since gradients in temperature naturally give rise to gradients in electron density which in turn result in electric fields. 3. It is necessary to assume an equation of state which relates pressure, density, and temperature. Regarding the first point, we focus our kinetic theory predictions on hydrogen plasmas at sufficiently weak coupling that we can neglect the potential energy contributions to the energy current; as such, we take the energy current to be $\mathbf{j}_Q = \int d^3v \frac{1}{2} m v^2 \mathbf{v} f(v)$. Regarding point 3, it can be shown that the thermal conductivity we seek, $K_{\rm th}$, can be computed either at constant electron density or at constant pressure, giving identical results [28], as long as the ideal gas assumption is made, $P = k_{\rm B} T/V$. This is in turn consistent with the assumption of weak plasma coupling.

The simplest treatment of collisions in a kinetic theory framework is the binary collision approximation, in which the total collision term is represented as the sum of independent 2-body scattering events. This picture, while attractive for developing a basic understanding, fails to address the most subtle aspect of plasma transport: the effect of screening on Coulomb collisions. Indeed, the very determination of the scattering time for a system of particles interacting via long-ranged Coulomb forces is a difficult one, requiring the concept of screening to mitigate the divergences which otherwise arise when the Coulomb cross-section is summed appropriately over impact parameter to produce $C[f]$. This famous problem was first addressed by Landau in 1936 [14] in the context of temperature equilibration in a 2-temperature classical Coulombic system. His solution made use of the realization that the dominant contribution to the energy exchange rate between two species of Coulombic particles is due to the many small-angle collisions with large impact parameters, but that once the impact parameter exceeds the screening length, the contribution drops to zero. This line of thinking produced a scattering time proportional to the reciprocal of the so-called Coulomb logarithm: $\ln \lambda \equiv \ln(b_{\rm max}/b_{\rm min})$, where $b_{\rm max}$ is taken to be a (static) Debye screening length, and $b_{\rm min}$ is a distance of closest approach (also termed the Landau length for a classical plasma). In the quantum fusion-burning plasmas which are our primary

interest here, it is more appropriate to set $b_{\min} = \lambda_{\rm dB}$, the thermal de Broglie wave length, as discussed in numerous previous works [4–6, 23]. The identification $b_{\min} = \lambda_{\rm dB}$ reflects the fact that electron wave packets with a spatial extent $\sim \lambda_{\rm dB}$ scatter through smaller angles than point-like electrons undergoing Kepler orbits [29].

Though this strategy of regularizing the logarithmic divergences appearing in Coulomb scattering calculations by imposing cutoffs is intuitively appealing, its limitations are severe. There are at least two reasons for this: 1. It manifestly only addresses weak plasma coupling, where small-angle collisions are dominant. 2. It invokes a notion of *static* screening in the identification of its $b_{\max}$; for each effective 2-body collision, it is necessary to identify those particles in the background plasma which are assumed to respond instantaneously to screen the inter-particle interaction in question, neglecting all others. For many real plasmas, these idealizations are inappropriate, however for the bulk of the hydrogen plasmas in this study, they provide a very reasonable starting-point.

There are two general families of (both quantum and classical) kinetic theories for plasma transport: Those which make use of ad hoc cutoffs in their representation of the logarithmic factors ($\ln \lambda$) which contribute to the scattering cross sections, and those which do not. Those invoking Coulomb-logs with cutoffs include the pioneering work of Spitzer and Härm [13], and Cohen, Spitzer, and Routly [30]. By extension, this set also includes the efforts which focus on constructing wide-ranging analytic models for plasma transport for fusion and related applications: Lee-More [4], Rinker [5], and Lee-More-Desjarlais [6], since a $\ln \lambda$-based description is entirely natural in the context of analytic expressions for both σ and $K_{\rm th}$. The theories not making use of truncated Coulomb-logs are those which take into account plasma screening explicitly, and therefore compute the collision term without the need for ad hoc (though physically motivated) cutoffs. There are two main variants of these: a. approaches based on the Ziman resistivity formula [31–33], in which $1/\tau$ is computed due to electron waves scattering off a collection of fixed ions dressed by background electrons, and b. Lenard-Balescu [23] approaches, where the integrand of $C[f]$ involves factors such as $\phi(\mathbf{q})/\epsilon(\mathbf{q}, \omega(\mathbf{q}))$, where $\phi(q)$ is the Fourier transform of the inter-particle interaction and ϵ is the wave vector-dependent and frequency-dependent dielectric function in the random phase approximation (RPA). Inclusion of ϵ in $C[f]$ regularizes the problem so that the cutoff, $b_{\max}$, in the Coulomb-logs is unnecessary. In both approaches, the disordered potential produced by the ions and felt by the electrons enters through an ion structure factor, S_{ii}.

Accompanying the details of the Coulomb collision physics, there is an associated effect which pertains to the *shape* in **v**-space of the steady-state electron distribution function, $f(\mathbf{v})$. As we noted above, the spherically-symmetric equilibrium distribution, f_0, contributes nothing to the (charge or energy) current, so the precise a-sphericity is therefore responsible for the magnitudes of σ and $K_{\rm th}$. This shape is the result of an interplay between the tendency for the electron-electron and electron-ion scatterings to make the distribution more isotropic, and the opposing tendency for the spatial gradients (due either to $\mathbf{E}$ or to $\nabla_{\mathbf{r}}T$) to cause it to elongate along a given direction. This reshaping of f can be studied by expanding f in orthogonal polynomials in the solution of Eq.4, as discussed in Refs.[28] and [13] for instance. For the case of nearly degenerate electrons, it turns out that a single polynomial suffices for σ, resulting in a solution which takes on a particularly simple form: the shifted distribution assumption [27], $f(v) = f_0(\mathbf{v} - [\mathbf{j}_Z/ne])$. For more general cases, the solution depends in a subtle way on the relative importance of electron-ion and electron-electron collisions, as discussed in Braginskii [34]. The degree of sophistication of this aspect of the treatment is independent of whether or not truncated Coulomb-logarithm assumptions are invoked. Spitzer-Härm [13] includes this effect in detail for both σ and $K_{\rm th}$, while the Ziman formula theories [32, 33] make the shifted-distribution approximation, thereby requiring multiplicative corrections (so-called "Lorenz gas corrections") to yield comparable results in this sense. Such corrections can be derived by taking the ratio of the infinite-polynomial result to the appropriate few-polynomial result, and are known to be more important for low-Z plasmas at high-T [34, 35].

In Spitzer-Härm [13] and Cohen-Spitzer-Routly [30], σ and $K_{\rm th}$ for a classical Coulomb plasma are predicted using what amounts to a Fokker-Planck equation addressing small-angle scattering (and therefore weak plasma coupling). The effect of the reshaping of $f(\mathbf{v})$ due to the electron-electron interaction is included. Coulomb-logs, $\ln\lambda_{\rm ee}$ and $\ln\lambda_{\rm ei}$, are assumed in which $b_{\rm max}$= a static Debye screening length, and $b_{\rm min}$= the classical distance of closest approach, $Ze^2/(k_{\rm B}T)$ for electron-ion [13]. These works still form the basis for what is currently understood about linear transport in a classical weakly-coupled system of particles interacting via the Coulomb interaction. It is reasonable to assume that analogous results for the quantum plasma can be obtained by simply replacing $b_{\rm min} = Ze^2/(k_{\rm B}T)$ by $b_{\rm min} = \lambda_{\rm dB}$. The theory of Williams and DeWitt [36] addresses small-angle scattering in a quantum-Coulomb plasma with a Lenard-Balescu scheme [23]. Here, the inclusion

of the 2-component homogeneous plasma dielectric function eliminates the need for the $b_{\max}$ of the Coulomb logarithm, while a proper accounting of quantum diffraction through the 2-body cross sections and the quantum density-density response eliminates the need for a $b_{\min}$. The full reshaping of f is included through a polynomial expansion. What is not included is the full antisymmetry of the many-electron wave function; rather, Pauli exclusion is accounted for only at the 2-body level, pertaining to the binary scattering of two electrons. In this sense, the global particle statistics must be Maxwellian, as is approximately the case for fusion-burning hydrogen, for example. This theory, together with later applications of it [37] constitute much of what is known about linear transport in hot (i.e., non-degenerate), weakly-coupled hydrogen plasmas. A theory addressing the full range of electron degeneracy is that of Ichimaru and Tanaka [38], in which a simplified version of the Lenard-Balescu prescription is derived which makes an explicit connection to forms culled from the Ziman resistivity formula [31]. This result, however, does not include a full treatment of the reshaping of the electron distribution function, and therefore is only strictly applicable at low-T, absent additional multiplicative corrections. Further work using the Ziman formula and approximate forms for the effective electron-ion potential and the ion structure factor have been used to predict transport in (partially ionized) high-Z plasmas [32, 33]. These also require reshaping corrections at high-T .

In what follows, we sketch our scheme for solving the Lenard-Balescu equation for a two-component plasma. Though, like Williams and DeWitt [36], we confine our interest to cases in which the unperturbed plasma particles obey Maxwellian statistics, we construct two such schemes: 1. Classical-LB and 2. Quantum-LB. In classical-LB, the classical dielectric response is assumed and the inter-particle interactions are taken to be QSPs, regularized around $r = 0$; this allows us to model our classical QSP-MD. In quantum-LB, we use the quantum dielectric response and the pure Coulomb inter-particle interactions; this is simply our version of Williams and DeWitt [36, 39] and Morales et al. [37], aimed at checking their findings and applying their approaches to the cases of our specific interest. Comparisons between classical-LB and QSP-MD predictions of σ and $K_{\rm th}$ will show that detailed features in the MD are represented extremely well by the theory. Comparisons between classical-LB and quantum-LB then allow us to determine, for these hydrogen plasmas, the optimal classical-QSP scheme for representing transport in quantum hydrogen.

B. Our Lenard-Balescu Approach

Considering first the quantum-Coulomb plasma, we seek the static solution to Eq.4 for the electron distribution, f_e,

$$\mathbf{v}\cdot\frac{\partial}{\partial\mathbf{r}}f_e(\mathbf{r},\mathbf{v})+\frac{\boldsymbol{F}}{m_e}\cdot\frac{\partial}{\partial\mathbf{v}}f_e(\mathbf{r},\mathbf{v})=C_{QLB}^{(ee)}(f_e)+C_{QLB}^{(ep)}(f_e)\ , \tag{6}$$

where $C_{QLB}(f)$ is the quantum Lenard-Balescu collision operator, although it was first derived by Wyld and Pines [40]. For electron-electron scattering the operator is

$$\begin{aligned} C_{QLB}^{(ee)}(f_e) \ &= \ -\frac{1}{4\pi^2\hbar^2}\int d^3\mathbf{v}'\int d^3\mathbf{q}\frac{|\phi_{ee}(q)|^2}{\left|\epsilon\left(q,\mathbf{q}\cdot\mathbf{v}+\frac{\hbar q^2}{2m_e}\right)\right|^2} \\ &\times\ \delta[\mathbf{q}\cdot(\mathbf{v}-\mathbf{v}')+\hbar q^2/m_e][f_e(\mathbf{v})f_e(\mathbf{v}')-f_e(\mathbf{v}+\hbar\mathbf{q}/m_e)f_e(\mathbf{v}'-\hbar\mathbf{q}/m_e)]\ . \end{aligned} \tag{7}$$

Since we are considering plasmas which are approaching the fusion-burning regime, we neglect the additional terms for $C_{QLB}^{(ee)}$ which involve the Pauli blocking factors, $1-f_e$ [41]. This is additionally appropriate because our primary motivation is to compare LB and classical MD. Within this same framework, the electron-proton collision term is

$$\begin{aligned} C_{QLB}^{(ep)}(f_e) \ &= \ -\frac{1}{4\pi^2\hbar^2}\int d^3\mathbf{v}'\int d^3\mathbf{q}\frac{|\phi_{ep}(q)|^2}{\left|\epsilon\left(q,\mathbf{q}\cdot\mathbf{v}+\frac{\hbar q^2}{2m_e}\right)\right|^2} \\ &\times\ \delta[\mathbf{q}\cdot(\mathbf{v}-\mathbf{v}')+\hbar q^2/2\mu][f_e(\mathbf{v})f_p(\mathbf{v}')-f_e(\mathbf{v}+\hbar\mathbf{q}/m_e)f_p(\mathbf{v}'-\hbar\mathbf{q}/m_p)]\ , \end{aligned} \tag{8}$$

where $\mu=m_em_p/(m_e+m_p)$ is the reduced mass. For the dielectric function appearing in these collision terms, we use the random phase approximation for two components [25]

$$\epsilon(q,\omega)=[1-\phi_{ee}(q)\chi_e(q,\omega)][1-\phi_{pp}(q)\chi_p(q,\omega)]-\phi_{ep}(q)^2\chi_e(q,\omega)\chi_p(q,\omega)\ , \tag{9}$$

where $\chi_\sigma(q,\omega)$ is the free-particle density-density response function for species σ and $\phi_{\sigma\sigma'}(q)$ is the Fourier transform of the σ-σ' interaction. These response functions are given by

$$\chi_\sigma(q,\omega)=\int d^3\mathbf{v}\frac{f_\sigma^{(0)}(\mathbf{v})-f_\sigma^{(0)}(\mathbf{v}+\hbar\mathbf{q}/m_\sigma)}{\hbar\omega-\hbar\mathbf{v}\cdot\mathbf{q}-\frac{\hbar^2q^2}{2m_\sigma}+i\eta}, \tag{10}$$

where η is a positive infinitesimal.

We construct perturbative solutions to Eq.6 to lowest order in $\mathbf{E}$ and ∇T:

$$f_e(\mathbf{r},\mathbf{v})=f_e^{(0)}(\mathbf{r},\mathbf{v})+f_e^{(1)}(\mathbf{v}), \tag{11}$$

where the unperturbed state is a spatially-dependent Maxwellian with a temperature gradient,

$$f_e^{(0)}(\mathbf{r},\mathbf{v}) = n_e \left(\frac{m_e\beta(\mathbf{r})}{2\pi}\right)^{3/2} e^{-m_e\beta(\mathbf{r})v^2/2}, \tag{12}$$

and $f_e^{(1)}$ is linear in $\mathbf{E}$ and ∇T. The perturbation, $f_e^{(1)}$, is then expanded in associated Laguerre (Sonin) polynomials [28, 36, 37, 42, 43]. The conductivities, σ and $K_{\rm th}$, are then related to the non-spherical parts of f_e. The determination of $f_e^{(1)}$ is considerably involved, particularly in the case of $K_{\rm th}$. Thus, we do not reproduce our lengthy expressions here, but exhibit them instead in an upcoming manuscript [12].

For the classical plasma, we take the $\hbar \longrightarrow 0$ limit of our expressions for the quantum case and (given our interest here in making comparisons with our MD simulations) replace the bare Coulomb interactions of ϕ_{ee} and ϕ_{ep} by the appropriate QSPs; in some cases, to be discussed in Section III, ϕ_{ee} includes both a diffractive piece and a 2-body Pauli term [51]. The essential differences between classical and quantum-LB results from the quantum vs. classical versions of Eqs.7,8,10: In the quantum case, the short-distance (large-q) logarithmic divergences are eliminated by the effect of quantum diffraction at large q, while for the classical case, the divergence is eliminated instead by the large-q behavior of the QSPs entering ϕ_{ee} and ϕ_{ei}. This is in direct correspondence to our previous quantum-Coulomb vs. classical-QSP LB calculations of temperature equilibration [1]. We note that our quantum-Coulomb LB calculations are essentially identical to those of Williams and DeWitt [36], though without the Boltzmann operator scattering term that they use to treat hard collisions in more strongly-coupled plasmas.

Because the quantum-LB approach we employ here includes in a natural way the effects of quantum diffraction and uses Coulomb interactions (rather than QSPs) for ϕ_{ee} and ϕ_{ei}, it is expected to give correct predictions as long as: 1. the electrons are non-degenerate, and 2. the plasma is sufficiently weakly-coupled for small-angle scattering to dominate [29].

III. SIMULATION METHOD

We use classical MD with QSPs to simulate hydrogen in various conditions of temperature and density in which the electrons are essentially non-degenerate. Since the main focus of this work, however, is to perform comparisons between MD and Lenard-Balescu (LB) calculations for linear transport, slight incursions into partially degenerate regimes are to be tolerated;

as long as we are comparing classical MD to classical-LB, both with the same assumed inter-particle interactions, the comparison is meaningful. We note that in contrast to our LB treatment, the MD scheme we employ below includes the (however small) contributions from the ions to the conductivities as well, since we perform simulations in which both species are treated dynamically, rather than averaging over snapshots of fixed ionic configurations.

We use the relations given above as Eqs.1, 2, and 3, to define σ and $K_{\rm th}$ and their dependences on the Onsager coefficients, L_{ZZ}, L_{QZ}, and L_{QQ}. We compute these Onsager coefficients from current-current correlation functions by appealing to the Kubo relations [22]:

$$\begin{aligned} L_{ZZ} &= \frac{1}{3k_BVT}\int_0^\infty \langle \mathbf{j}_Z(t)\cdot\mathbf{j}_Z(0)\rangle dt, \\ L_{QZ} &= \frac{1}{3k_BVT^2}\int_0^\infty \langle \mathbf{j}_Q(t)\cdot\mathbf{j}_Z(0)\rangle dt, \\ L_{QQ} &= \frac{1}{3k_BVT^2}\int_0^\infty \langle \mathbf{j}_Q(t)\cdot\mathbf{j}_Q(0)\rangle dt, \end{aligned} \tag{13}$$

where V is the volume of the system, and T is the temperature.

The computation of the correlation functions in Eqs.13 is quite challenging, as has been discussed by other authors [44–47] and by us in an upcoming manuscript [12]. This is because the long-time behavior requires a long MD simulation which is difficult to perform with sufficient accuracy when small MD time-steps are required. In addition, we find that for system sizes of between 10^4 and 10^5 particles, the computed conductivities vary by 20% for σ and by 30% for $K_{\rm th}$ for statistically independent initial configurations. For the energy current, $\mathbf{j}_Q$, we take into account both the kinetic energy piece ($\propto \sum_{\rm particles} \frac{1}{2}mv^2\mathbf{v}$), and the potential energy piece possessing virial terms which we evaluate using the Ewald method of Galamba et al. [48]. In this sense, our MD description is capable of handling strong coupling, in contrast to the Lenard-Balescu approach we use and discuss above for which $\mathbf{j}_Q$ includes only the kinetic piece. However, we will see below that for the fairly weakly-coupled systems we consider here, reasonable quantitative agreement between our LB and MD results is obtained. The forces and potential energies needed for our MD computations of σ and $K_{\rm th}$ are evaluated with the aid of the particle-particle, particle-mesh method [49, 50].

Prior to accumulating MD data used to compute the conductivities, we initialize our systems by assigning random particle positions with the particle velocities sampled from a Maxwellian at the chosen T. Equilibration is affected by initially setting $m_{\rm proton} = m_{\rm electron}$

and equilibrating with a Langevin thermostat [49], after which $m_{\rm proton}$ is rescaled to its physical value and the proton velocities are rescaled so as to preserve the total kinetic energy. The thermostat is then turned off and the system is allowed to evolve micro-canonically while the correlation functions of Eqs.13 are computed. The MD time-steps are chosen to converge the total energy to within 0.001 eV/fs per particle, which yields time-steps in the neighborhood of 10^{-5} fs. Charge and energy currents are evaluated roughly every 10 MD time-steps.

As mentioned variously above, we use QSPs for all of our MD studies reported here. In such classical inter-particle potentials, the effects of quantum diffraction are accounted for approximately by applying corrections which soften the otherwise Coulombic interactions within a range given by the thermal de Broglie wave lengths (the ϕ_{pp} interaction is essentially purely Coulombic here, since we consider temperatures for which the proton de Broglie length is much smaller than the proton-proton classical distance of closest approach). We consider two types of diffractive QSPs, each derived by requiring that various static properties of quantum hydrogen at elevated temperature are reproduced in classical simulations: Dunn-Broyles [16] and modified-Kelbg [15, 18, 19]. We choose to perform the bulk of our simulations with Dunn-Broyles because it is in relatively wide use; its form is

$$U(r_{ij},\beta) = \frac{q_i q_j}{r_{ij}}\left[1 - e^{-\frac{r_{ij}\pi}{\lambda_{ij}}}\right], \tag{14}$$

where $\lambda_{ij} = \hbar/\sqrt{2\mu_{ij}k_{\rm B}T}$ and μ_{ij} is the reduced mass for particles of type i and j. The Kelbg diffractive term also involves λ_{ij} [15],

$$U(r_{ij},\beta) = \frac{q_i q_j}{r_{ij}}\left[1 - e^{-\left(\frac{r_{ij}}{\lambda_{ij}}\right)^2}\right] + \sqrt{\pi}\frac{q_i q_j}{\lambda_{ij}}\left[1 - \mathrm{erf}\left(\frac{r_{ij}}{\lambda_{ij}}\right)\right]. \tag{15}$$

In addition, we also explore the use of a correction to $\phi_{\rm ee}$ to account for Fermi statistics. This so-called Pauli term is the one employed by Deutsch, Minoo, and Gombert [51]

$$U_{ee}(r_{ij},\beta) = \beta^{-1}\ln(2)\exp\left(-[\pi\ln(2)]^{-1}r^2/\Lambda_H^2]\right), \tag{16}$$

where $\Lambda_H = \hbar/\sqrt{\pi m_e T}$. We will see below that the effect of this term is exceedingly large especially for $K_{\rm th}$, and that comparisons to various quantum Lenard-Balescu theory results suggest that its use for thermal transport should probably be avoided particularly in weak-coupling. However, for static quantities like total energies and static structure factors,

inclusion of this term does indeed produce improvements when comparing to path integral Monte Carlo simulations [17]. Other effective 2-body Pauli terms constructed with different philosophies exist [52, 53], but are essentially almost indistinguishable with that of Eq.16 for the conditions of our interest.

IV. DISCUSSION OF RESULTS: COMPARISONS BETWEEN THEORY AND SIMULATION

Our QSP-MD calculations of σ and $K_{\rm th}$ for hydrogen involve simulations with 10,000 particles (5000 electrons + 5000 protons) in a periodic cell with a size appropriate for the chosen density using the massively-parallel ddcmd code [17, 54]. Table I displays results obtained with QSPs of the Dunn-Broyles form for the diffractive piece + the 2-body Pauli term as introduced in Ref.[51]. Note that for fixed density, σ and $K_{\rm th}$ increase as T increases, as predicted for non-degenerate electrons by various theories [13, 30, 36–38]. Table II shows a smaller set of results with $\rho = 40$ g/cc, from QSP-MD using the Dunn-Broyles diffractive term and *without* the addition of the Pauli potential. We see that while σ is increased slightly if the Pauli term is discarded, $K_{\rm th}$ is increased substantially. The Pauli term adds an extra repulsion which further reduces the electronic (charge and energy) current. The fact that this reduction is larger for $K_{\rm th}$ than for σ is to be expected: Two-body electron-electron scattering alone does nothing to alter the electrical current, since $\mathbf{j}_Z$ is proportional to the total electron momentum, which is conserved. This does not apply to the energy current, since $\mathbf{j}_Q \propto v^3$. In an upcoming manuscript [12], we show that much of this large dependence of $K_{\rm th}$ on the Pauli term can be understood by analyzing the partial-wave decomposition of the relevant scattering cross section. Our comparison (below) to quantum-Coulomb LB will suggest that the inclusion of a 2-body Pauli term for hydrogen conductivities in this regime is in fact suspect.

These QSP-MD results for σ and $K_{\rm th}$ are largely reproduced in our classical-QSP LB calculations. Figure 1 shows σ vs. T for hydrogen as computed by QSP-MD (symbols) and classical-LB (lines; identical colors) with the identical QSPs and the scheme outlined in Section II B. The open symbols indicate the results for individual MD replicas, while the corresponding filled symbols at the same T show their arithmetic averages, reproduced in Tables I and II. The solid brown curve shows the conductivity as computed by the Purgatorio

Density (g/cc)	Temperature (eV)	σ (Ohm m)$^{-1}$	$K_{\rm th}$ (W/(K m)
2.66	27	1.20e7	2.21e4
2.66	54	1.46e7	4.9e4
10.0	86	4.00e7	3.0e5
10.0	172	5.00e7	5.0e5
40.0	500	1.725e8	3.8e6
40.0	700	2.025e8	8.8e6
40.0	900	2.50e8	1.1e7

TABLE I: QSP-MD results for electrical and thermal conductivities of hydrogen plasmas at various conditions. Here, the QSPs used are Dunn-Broyles [16] for the diffractive piece and the prescription of Ref.[51] for the Pauli term. Each value represents an average over multiple statistically independent replicas.

Density (g/cc)	Temperature (eV)	σ (Ohm m)$^{-1}$	$K_{\rm th}$ (W/(K m)
40.0	500	2.05e8	1.0025e7
40.0	700	2.564e8	2.50e7
40.0	900	3.227e8	3.363e7

TABLE II: QSP-MD results for electrical and thermal conductivities of hydrogen plasmas at various conditions. Here, the QSPs used are Dunn-Broyles [16] for the diffractive piece and *no* Pauli term. Each value represents an average over multiple statistically independent replicas.

model [32] which we alluded to in Section II A. The differences between Dunn-Broyles + Pauli (magenta) and Dunn-Broyles without Pauli (cyan) are strikingly similar in both LB and MD, and the absolute magnitudes, simulation vs. theory, are also quite close. This is also seen in the analogous comparison for $K_{\rm th}$ (see Fig.2) where the Pauli/no-Pauli difference is considerably larger. In addition, we also present classical-QSP LB results for cases in which the diffractive terms in ϕ_{ee} and ϕ_{ep} are chosen to be of the Kelbg form [15] (solid black line for Kelbg + Pauli; dashed black line for Kelbg + no Pauli). These produce somewhat lower conductivities than those using Dunn-Broyles. The general agreement between simulation and theory for the Dunn-Broyles cases shows that for these plasma conditions (and for

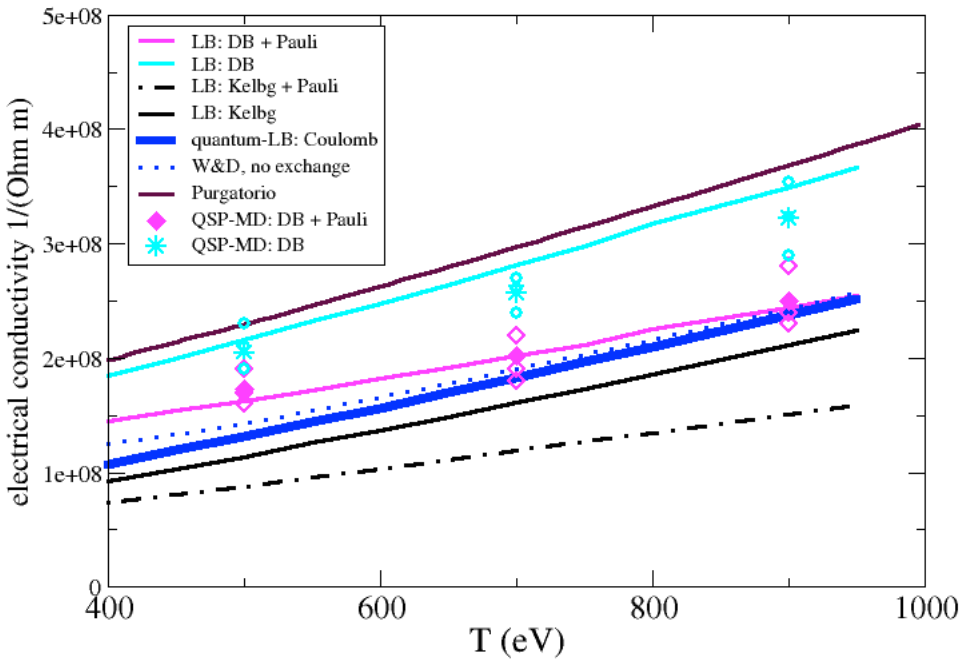

FIG. 1: Electrical conductivities of hydrogen plasmas with $\rho = 40$ g/cc. Magenta symbols (curve) are QSP-MD (classical-LB) with the Dunn-Broyles diffractive term + the Pauli correction; cyan symbols (curve) are QSP-MD (classical-LB) with Dunn-Broyles and *no* Pauli term. The open symbols showing a range of values for each T indicate the results for individual MD replicas. The dot-dashed black curve is classical-LB with the modified-Kelbg [15] diffractive term + Pauli; solid black curve is classical-LB with modified-Kelbg and *no* Pauli term. The dark blue curve is quantum Lenard-Balescu using the bare Coulomb interaction; dotted blue curve is the result of the quantum-Coulomb LB approach of Williams and DeWitt [36] without their exchange correction. The solid brown curve shows the Purgatorio (DFT average-atom-in-jellium) [32] result.

the QSPs used), the small-angle scattering and linear screening assumptions inherent in Lenard-Balescu theory are generally satisfied. It is then natural to ask: a. How well does this classical-QSP hydrogen represent true quantum hydrogen? b. Which choice of QSPs is expected to be best for modeling electrical and thermal transport in nature's quantum hydrogen plasma?

We address these questions by comparing to our quantum-Coulomb LB results for hy-

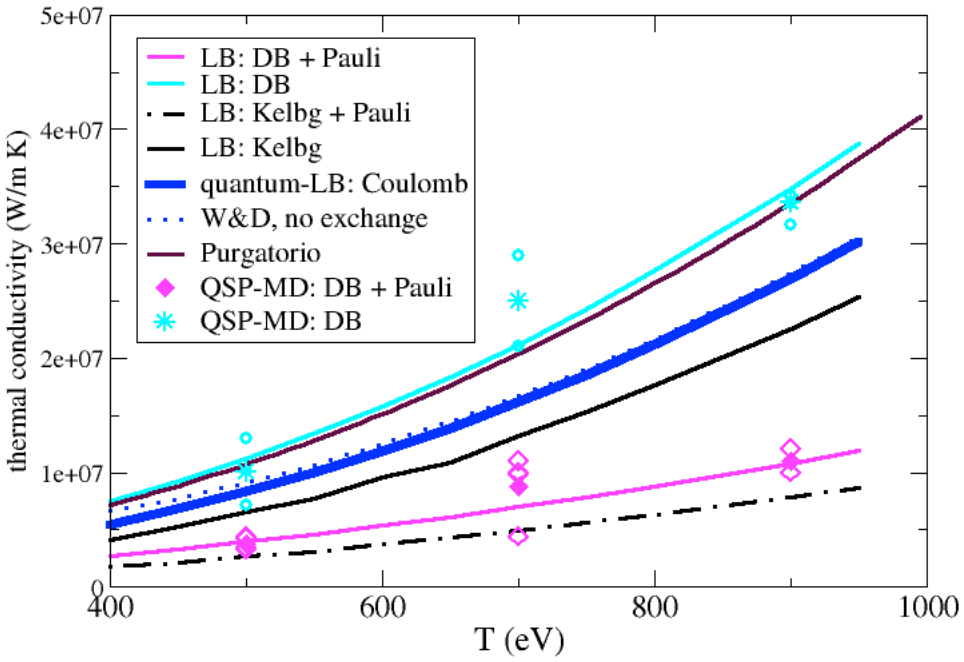

FIG. 2: Thermal conductivities of hydrogen plasmas with $\rho = 40$ g/cc. Magenta symbols (curve) are QSP-MD (classical-LB) with the Dunn-Broyles diffractive term + the Pauli correction; cyan symbols (curve) are QSP-MD (classical-LB) with Dunn-Broyles and *no* Pauli term. The open symbols showing a range of values for each T indicate the results for individual MD replicas. The dot-dashed black curve is classical-LB with the modified-Kelbg [15] diffractive term + Pauli; solid black curve is classical-LB with modified-Kelbg and *no* Pauli term. The dark blue curve is quantum Lenard-Balescu using the bare Coulomb interaction; dotted blue curve is the result of the quantum-Coulomb LB approach of Williams and DeWitt [36] without their exchange correction. The solid brown curve shows the Purgatorio (DFT average-atom-in-jellium) [32] result.

drogen in the same conditions, shown as the blue solid lines in Figs.1 and 2. These curves are very similar to those generated by our evaluation of the theory of Williams and DeWitt [36] for these conditions (dotted blue lines), though our quantum-LB lacks both the hard-scattering (Boltzmann) term and the correction to the Coulomb scattering cross section from 2-body exchange [39, 55]. Comparisons between our classical and quantum Lenard-Balescu results indicate that the best agreement is obtained when: 1. The diffractive pieces of the

QSPs are chosen to be of the Kelbg form [15], rather than Dunn-Broyles, and 2. The 2-body Pauli term for electron-electron is set to zero. We note that our prior work supports the first conclusion: in Ref.[1], we demonstrated that the use of the Kelbg diffractive potential in a classical MD calculation is the nearly optimal choice for reproducing energy exchange rates for quantum weakly-coupled 2-T hydrogen plasmas. Since energy exchange is closely related to resistive heating, it can also be motivated using both classical and quantum variants of the theory of Ichimaru and Tanaka [38] that the Kelbg diffractive form should be the optimal choice for σ and $K_{\rm th}$ as well. The second conclusion is consistent with the findings of earlier studies [46, 56]; a detailed discussion of the unphysically large effect of the Pauli term on $K_{\rm th}$ at high T appears in an upcoming work [12]. As a final illustration of these points, we note that our classical LB results for this same density represented in Figs.1 and 2 ($\rho = 40$ g/cc), but at the much higher temperature of 10,000 eV, show the ratio $K_{\rm th}$(Kelbg, no Pauli)/$K_{\rm th}$(Kelbg + Pauli) to be 8.22, while σ(Kelbg, no Pauli)/σ(Kelbg + Pauli) = 1.74. The effect of the Pauli term therefore remains especially large for $K_{\rm th}$ even at exceedingly weak coupling, and we find that the Kelbg-without-Pauli $K_{\rm th}$ is considerably closer to the quantum-LB result than are Kelbg + Pauli or Dunn-Broyles + Pauli.

V. CONCLUSIONS

We discussed the development of kinetic theories for the prediction of electrical and thermal conductivities of dense plasmas, and have applied a particular variant, Lenard-Balescu theory, to hydrogen plasmas with 2 g/cc $< \rho <$ 40 g/cc and 20 eV $< T <$ 900 eV. In addition, we presented equilibrium classical MD simulations of the same quantities in which various combinations of 2-body quantum statistical potentials were used to model quantum diffraction in the Coulomb scattering processes. Evaluation of $K_{\rm th}$ using both quantum-Coulomb and classical-QSP Lenard Balescu theory allowed us to conclude that the Kelbg diffractive piece is likely better to use than the Dunn-Broyles equivalent, and that the use of a correction to ϕ_{ee} to handle the effects of partial degeneracy has a large effect which pushes the thermal conductivity away from the best available quantum kinetic theory predictions at weak coupling.

We are now in a position to compare both types of calculations to DFT-MD predictions of σ and $K_{\rm th}$ for hydrogen plasmas. Further details along these lines are forthcoming [12]. In

addition, the MD component of this work should inform future studies of thermal transport in situations where ∇T is large enough to preclude the possibility of appealing to the linear response paradigm. Such situations are indeed thought to be of importance in ICF [2].

VI. ACKNOWLEDGEMENTS

We thank J.C. Weisheit, W.H. Cabot, L.G. Stanton, R. Redmer, M.S. Murillo, P.E. Grabsowski, and M. Bonitz for helpful discussions. H.D. Whitley is grateful to the DOE for support provided through a PCASE Award. This work was performed under the auspices of the U.S. Department of Energy by Lawrence Livermore National Laboratory under Contract No. DE-AC52-07NA27344. This work was funded by the Laboratory Directed Research and Development Program at LLNL under tracking code No. 12-SI-005.

[1] L.X. Benedict et al., Phys. Rev. E **86**, 046406 (2012).

[2] D.S. Clark, S.W. Haan, B.A. Hammel, J.D. Salmonson, D.A. Callahan, R.P.J. Town, *Phys. Plasmas*, **17**, 052703 (2010); S.W. Haan, J.D. Lindl, D.A. Callahan et al., Phys. Plasmas, **18**, 051001 (2011).

[3] B.A. Hammel et al., High Ener. Dens. Phys. (2010), doi:10.1016/j.hedp.2009.12.005.

[4] Y.T. Lee and R.M. More, Phys. Fluids **27**, 1273 (1984).

[5] G.A. Rinker, Phys. Rev. A **37**, 1284 (1988).

[6] M.P. Desjarlais, Contrib. Plasma Phys. **41**, 267 (2001).

[7] A.W. DeSilva and J.D. Katsouros, Phys. Rev. E **57**, 5945 (1986).

[8] J.F. Benage, W.R. Shanahan, and M.S. Murillo, Phys. Rev. Lett. **83**, 2953 (1999); J.F. Benage, Phys. Plasmas **7**, 2040 (2000).

[9] F. Lambert, V. Recoules, A. Decoster, J. Clerioun, and M.P. Desjarlais, Phys. Plasmas **18**, 056306 (2011).

[10] D.E. Hansen, L.A. Collins, J.D. Kress, and M.P. Desjarlais, Phys. Plasmas **18**, 082704 (2011).

[11] B. Holst, M. French, and R. Redmer, Phys. Rev. B **83**, 235120 (2011).

[12] M.P. Desjarlais, C.R. Scullard, H.D. Whitley, J.I. Castor, J.C. Weisheit, L.X. Benedict, A. Peters, J.N. Glosli, D.F. Richards, M.S. Murillo, and F.R. Graziani, unpublished (2014).

[13] L. Spitzer and R. Härm, Phys. Rev. **89**, 977 (1953).

[14] L.D. Landau, Phys. Z. Sowjetunion **10**, 154 (1936); Zh. Eksp. Teor. Fiz **7**, 203 (1937).

[15] G. Kelbg, Ann. Phys. **12**, 219 (1963).

[16] T. Dunn and A.A. Broyles, Phys. Rev. A **157**, 156 (1967).

[17] F.R. Graziani et al., High Ener. Dens. Phys. **8**, 105 (2012).

[18] A. Filinov, M. Bonitz, and W. Ebeling, and J. Phys. A **36**, 5957 (2003).

[19] A.V. Filinov, V.O. Golubnychiy, M. Bonitz, W. Ebeling, and J. W. Dufty, Phys. Rev. E **70**, 046411 (2004).

[20] J.P. Hansen and I.R. McDonald, Phys. Lett. A **97**, 42 (1983).

[21] B. Jeon, M. Foster, J. Colgan, G. Csanak, J.D. Kress, L.A. Collins, and N. Gronbech-Jensen, Phys. Rev. E **78**, 036403 (2008).

[22] R. Kubo, Rep. Prog. Phys. **29**, 255 (1966).

[23] A. Lenard, Ann. Phys. **10**, 390 (1960); R. Balescu, Phys. Fluids **3**, 52 (1960).

[24] S.R. De Groot and P. Mazur, *Non-equilibrium thermodynamics* (North-Holland Publishing Co., Amsterdam, 1962).

[25] S. Ichimaru *Statistical Plasma Physics, Vol.1: Basic Principles* (Addison-Wesley, Redwood City, CA, 1992).

[26] P.L. Bhatnagar, E.P. Gross, and M. Krook, Phys. Rev. **94**, 511 (1954).

[27] C. Kittel, *Introduction to Solid State Physics* (John Wiley and Sons, Inc., New York, 1995).

[28] S. Chapman and T.G. Cowling *The Mathematical Theory of Non-Uniform Gases*, 3rd ed. (Cambridge University Press, New York, 1970).

[29] L. Spitzer Jr., *The Physics of Fully Ionized Gases*, 2nd ed. (Interscience, New York, 1962).

[30] R.S. Cohen, L. Spitzer Jr., and P.M. Routly, Phys. Rev. **80**, 230 (1950).

[31] J.M. Ziman, Philos. Mag. **6**, 1013 (1961); J.M. Ziman, *Models of Disorder: The Theoretical Physics of Homogeneously Disordered Systems* (Cambridge University Press, New York, 1979).

[32] P.A. Sterne, S.B. Hansen, B.G. Wilson, and W.A. Isaacs, High Ener. Dens. Phys. **3**, 278 (2007).

[33] B.F. Rosznyai, High Ener. Dens. Phys. **4**, 64 (2008).

[34] S.I. Braginski, Zh Eksp. Teor. Fiz. **33**, 459 (1958).

[35] For high-Z plasmas, the effects resulting from the electron-electron interaction are outweighed by the larger electron-ion interaction.

[36] R.H. Williams and H.E. DeWitt, Phys. Fluids **12**, 2326 (1969).

[37] F. Morales, M.K. Kilmann, R. Redmer, M. Schlanges, and F. Bialas, Contrib. Plasma Phys. **29**, 425 (1989).

[38] S. Ichimaru and S. Tanaka, Phys. Rev. E **32**, 1790 (1985).

[39] Note that Williams and DeWitt [36] use a slightly different philosophy for the treatment of hard collisions which is based on the earlier work of H. Gould and H.E. DeWitt, Phys. Rev. **155**, 68 (1967). For the plasmas we study here, we find that such hard-collision corrections are unimportant.

[40] H.W. Wyld Jr. and D. Pines, Phys. Rev. **127**, 1851 (1962).

[41] D. Kremp, M. Schlanges, W.-D. Kraeft, and T. Bornath, *Quantum Statistics of Nonideal Plasmas*, (Springer-Verlag Berlin, Heidelberg, 2005).

[42] S. Kaneko, J. Phys. Soc. Jap. **15**, 1685 (1962).

[43] R. Landshoff, Phys. Rev. **76**, 904 (1949); ibid., Phys. Rev. **82**, 442 (1951).

[44] B. Bernu and J.P. Hansen, Phys. Rev. Lett. **48** 1375 (1982).

[45] B. Bernu and J.P. Hansen, Phys. Rev. Lett. **48**, 1375 (1985).

[46] V. Zehnlé, B. Bernu, and J. Wallenborn, J. Phys. France **49**, 1147 (1988).

[47] B. Bernu and P. Viellefosse, Phys. Rev. A **18**, 2345 (1978).

[48] N. Galamba, C.A.N. de Castro, and J.F. Ely, J. Chem. Phys. **120**, 8676 (2004).

[49] R.W. Hockney and J.W. Eastwood *Computer Simulation Using Particles* (McGraw-Hill, New York, 1981).

[50] E.L. Pollock and J.N. Glosli, Comp. Phys. Comm. **95**, 93 (1996).

[51] H. Minoo, M.M. Gombert, and C. Deutsch, Phys. Rev. A **23**, 924 (1981).

[52] G.E. Uhlenbeck and L. Gropper, Phys. Rev. **41**, 79 (1932).

[53] F. Lado, J. Chem. Phys. **47**, 5369 (1967).

[54] F.H. Streitz, J.N. Glosli, and M.V. Patel, Phys. Rev. Lett. **96**, 225701 (2006).

[55] We compare to the Williams and DeWitt [36] predictions which exclude their exchange correction to the scattering cross sections, since our quantum-LB treatment also excludes this physics. Their full results including this correction modifies the results shown here only very slightly in these conditions. Note also that while Williams and DeWitt include corrections (absent in our quantum-Coulomb LB treatment) to account for hard-scattering, their values for σ and $K_{\rm th}$ are nevertheless slightly *larger* than our quantum-LB results. We attribute this to various approximations they made which involve expansions in small parameters not made by us in this study.

[56] B. Bernu, J. Wallenborn, and V. Zehnlé, J. Phys. France **49**, 1161 (1988).